ORGANIC CHEMISTRY FRONTIERS

RESEARCH ARTICLE

View Article Online
View Journal | View Issue

Cite this: *Org. Chem. Front.*, 2021, **8**, 3668

Received 30th March 2021,
Accepted 29th April 2021

DOI: 10.1039/d1qo00478f

rsc.li/frontiers-organic

Cucurbitimines – imine cages with concave walls†

Christine Bourguignon, Dorothee Schindler,‡ Gangxiang Zhou, Frank Rominger and Michael Mastalerz *

The variety of shape-persistent organic cages by imine bond formation has tremendously enlarged in recent years by using different building blocks (aldehydes and amines) in the condensation reactions. Here, we describe the use of a kinked tetraldehyde to generate pumpkin-shaped cages with concave walls, similar to cucurbiturils.

Introduction

The synthesis of shape-persistent organic cage compounds, applying dynamic covalent chemistry (DCC) has developed in recent years tremendously fast and enabled the access of a large variety of defined molecular structures of different sizes, geometries and functions.[1–6] Although a few examples of boronic ester cages, or those based on disulphide formation or other DCC reactions are known,[7–18,19–21,22–26] no doubt, the vast majority of shape-persistent organic cages is relying on the use of multiple imine condensation reactions,[1] which bear the advantage to be transformed further to convert these to chemically robust cages,[27–31] which is for the other type of DCC reactions difficult or even impossible.[32] Among those imine cages, shapes, such as trigonal prisms,[33–35] tetrahedra,[36–39] truncated tetrahedra,[40,41] cubes,[42–46] tetrapods,[47] adamantoids[48–50] and even more complex structures[51–57] have been realized as well as tubular structures, based on linear tetraaldehydes.[58–61,62]

Here we introduce [3 + 6] imine cages based on the condensation of triptycene tetraaldehydes with 1,2-cyclohexyldiamines. Due to the inherent 120° angle of the triptycene blades, the resulting imine cage contains concave π-walls giving the overall structure the shape comparable to those of cucurbiturils,[63–67] thus we call the compounds cucurbitimines (Fig. 1).

Results and discussion

A key-step in the achievement of cucurbitimines is the synthesis of a triptycene-based tetraaldehyde precursor, having on two aromatic blades two aldehyde units each and at the third one none. Therefore, we developed a route where electron density of one blade was diminished by turning it into a phenazine unit and in addition allowed us to install long solubilizing hexyl-sidechains (Scheme 1). To achieve this first synthetic goal, hexamethoxytriptycene **1** was partially oxidized to the quinone **2**[68–70] and condensed with phenylene diamine **3**[71] to give phenazine **4** in 79% yield.[72] The next step is the introduction of the aldehyde groups. Finally, the tetraaldehyde precursor was achieved by a three-step-method, which was based on the fourfold chloromethylation to **5** (60% yield), followed by basic substitution of chlorine by hydroxyl groups to give

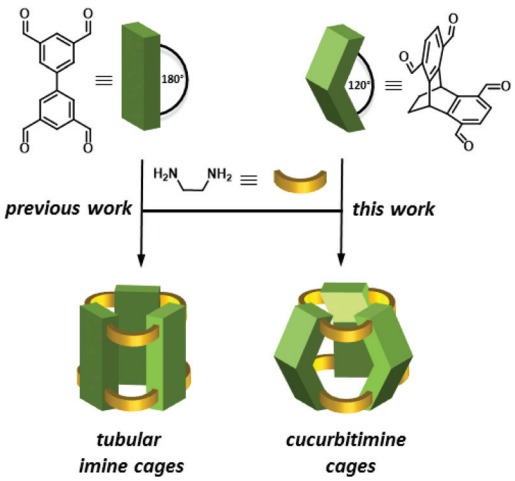

Fig. 1 Schematic representation of literature-known tubular [3 + 6] imine cages (left)[58–61] and the cucurbitimines presented herein. Please note that any further functional groups or substituents present in the molecular structures have been omitted for clarity.

Organisch-Chemisches Institut, Ruprecht-Karls-Universität Heidelberg, Im Neuenheimer Feld 270, 69120 Heidelberg, Germany.
E-mail: michael.mastalerz@oci.uni-heidelberg.de

†Electronic supplementary information (ESI) available. CCDC 2072797 (**4**), 2072798 (**5**), and 2072799 ((*R*,*R*)-**9**). For ESI and crystallographic data in CIF or other electronic format see DOI: 10.1039/d1qo00478f

‡Current address. Institut für Organische Chemie, Julius-Maximilians-Universität Würzburg, Am Hubland, 97074 Würzburg, Germany

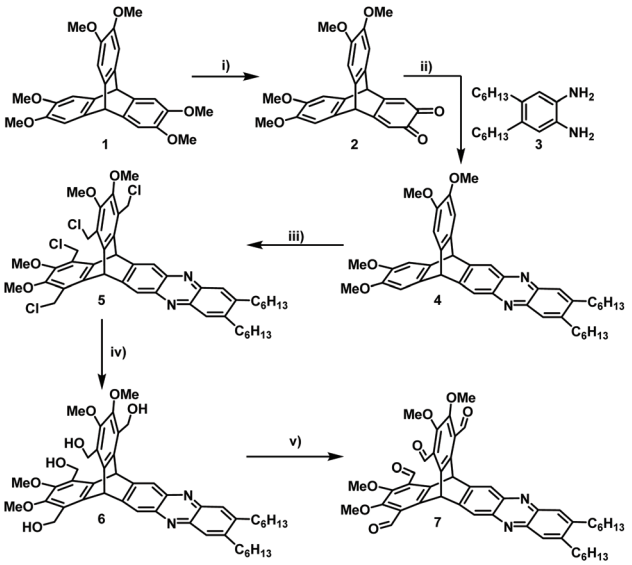

Scheme 1 Synthesis of tetraaldehyde **7**. (i) conc. HNO_3, DCM, AcOH, 5 min, 91%; (ii) $CHCl_3$, AcOH, 80 °C, 7 h, 79%; (iii) $ClCH_2OCH_3$, CH_3SO_3H, 80 °C, 16 h, 60%; (iv) Cs_2CO_3, dioxane/water (1 : 1 v/v), 140 °C, 3d, 77%; (v) PCC, Celite, DCM, r.t., 6 h, 85%.

tetra benzylic alcohol **6** in 77% yield, which was then oxidized with pyridinium chloro chromate (PCC) to give tetraaldehyde **7** in 85% yield. All compounds have been fully characterized, including single crystal structure analysis by X-ray diffraction for **4** and **5** (for details, see ESI†).

With tetraaldehyde **7** in hand, condensation reactions with (*R*,*R*)-1,2-cyclohexyldiamine **8** were investigated under various conditions (Scheme 2). Solvents, such as MeOH, MeCN, DCM, THF, toluene or $CHCl_3$ were used and the reactants with the addition of a small amount of TFA (2 mol%) were stirred at room temperature or under reflux. Although in all cases the [3 + 6] cucurbitimine cage was formed, as detected by MALDI-TOF mass spectrometry (*m*/*z* = 2739), the corresponding ^{1}H NMR spectra revealed that only in DCM the purity of the crude material was high enough to allow isolation and purification of the cage **9** in 10% yield. However, the best results were achieved by layering solutions of the two reactants and let them diffuse into each other, which has been widely used by Cooper *et al.*[37,73,74] Although in contrast to their cages, which usually crystallized during formation, here the reaction mixture still kept a clear solution. Nevertheless, by this method we were able to isolate cucurbitimine cage (*R*,*R*)-**9** in 49% yield by applying separation with recycling-GPC (gel permeation chromatography,) besides 5% of the larger [4 + 8] cage (*R*,*R*)-**10** (*m*/*z* = 3653). Using the enantiomeric (*S*,*S*)-1,2-cyclohexyldiamine gave basically the same results and here the cages (*S*,*S*)-**9** and (*S*,*S*)-**10** have been isolated in 54% and 5% yield (Fig. 2). It is worth to mention, that the calculated heats of formation (PM3) for the trimeric cage **9** is ΔH_f = 751 kJ mol^{-1} (250.3 kJ mol per unit) and for tetrameric cage **10** ΔH_f = 975 kJ mol^{-1} (243.3 kJ mol per unit) are very similar, if compared per unit ($\Delta\Delta H_f$ = 7 kJ mol^{-1}). Thus a more equal distribution would be excepted, if the cage products are in thermodynamically equilibrium. Since it is not the case in combination with all the observations made under various reaction conditions, it is concluded, that the cages **9** are rather kinetically controlled products than thermodynamically ones.

In the ^{1}H NMR spectra of enantiopure cages **9**, the most characteristic peaks are found in the aromatic region (Fig. 3). Whereas triptycene bridgehead protons overlap with the outer phenazine protons (7.84 ppm), the inner ones resonate at 7.67 ppm. The imine protons show a large difference in chemical shifts. The peak at 9.26 ppm are assigned to the imine protons closer to the triptycene bridgeheads, the peak at 8.70 ppm corresponds to the imine protons pointing towards the outer rim of the cage. The larger cages **10** are unfortunately not stable enough to be fully purified by GPC or other means and still contain some minor impurities, as detected by ^{1}H NMR spectroscopy (see ESI†). By DOSY experiments, diffusion

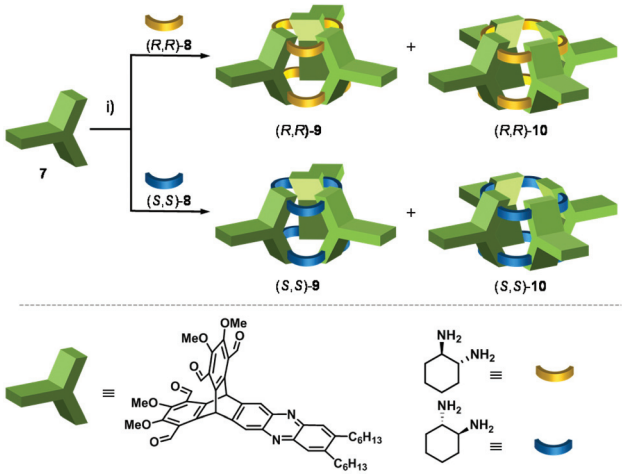

Scheme 2 Synthesis of cucurbitimines. (i) DCM, 2 mol% TFA, r.t., 7d, yields: (*R*,*R*)-**9** (49%); (*R*,*R*)-**10** (5%); (*S*,*S*)-**9** (54%); (*S*,*S*)-**10** (5%).

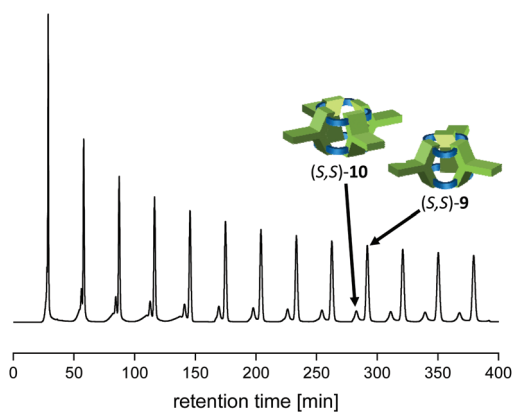

Fig. 2 Recycling-GPC chromatogram of the reaction of **7** with (*S*,*S*)-**8**. For experimental details, see ESI.† Please note that in between the peak at 150 min and 160 min, the compounds responsible for the broad peak were removed.

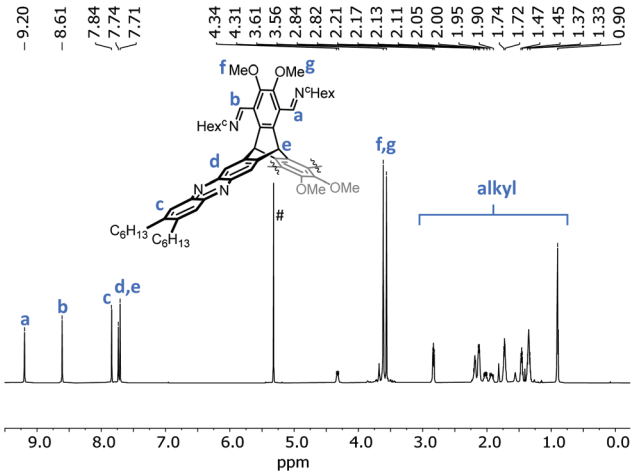

Fig. 3 ^{1}H NMR spectrum (700 MHz, CD_2Cl_2) of cage (*R,R*)-**9**. # residual CH_2Cl_2.

coefficients of $D = 4.3 \times 10^{-10}$ m^2 s^{-1} for the cages **9** were determined, which corresponds to a solvodynamic radius of r_s = 1.1 nm and fits well to the outer diameter of the molecule found by single-crystal X-ray diffraction (*vide infra*). For [4 + 8] cage **10** a diffusion coefficient of $D = 3.4 \times 10^{-10}$ m^2 s^{-1} was measured, thus the solvodynamic radius was a bit larger (r_s = 1.4 nm) and fits to the radius of the molecular model (see below).

For cage (*R,R*)-**9** single-crystals for X-ray diffraction were grown from diffusion of *n*-pentane into a saturated solution of the cage in DCM (Fig. 4). The compound crystallizes in the orthorhombic space group $P2_12_12$ and contained one enclathrated DCM molecule inside the cavity and disordered electron density (according to 8 DCM molecules per asymmetric unit) inside the formed extrinsic channels (Fig. 4d and e). The cages pack window-to-window with a closest distance of two methoxy units of *d*(C···OMe) = 3.47 Å (Fig. 4b), which is a hint for some week dipole–dipole interactions (Keesom interactions) as found before for methoxy-substituted π-extended heteroarenes.[75] Due to the relative small window, pores are isolated, *e.g.* for gases with kinetic diameters >2.2 Å, if one assumes a static structure in the crystals.[76] By the second dominant packing motif (CH···π interactions) between the cyclohexyl moieties and the aromatic phenazine backbones (Fig. 4c) extrinsic one-dimensional channels are formed containing disordered solvate (DCM) molecules (Fig. 4d and e). Up to now, these have not been tried to be activated for gas sorption, because we are more interested in the molecular structure as defined host for supramolecular host-guest chemistry.

It is worth to compare the molecular dimensions of the cavity of the cucurbitimines **9** with the cucurbiturils (Fig. 5). The distance between two oxygens of adjacent veratrole units is between 3.8 and 4.6 Å. The distance of two adjacent triptycene bridgehead carbons is 7.6 Å. The height of the molecule (distance between two eclipsed oxygens of the upper and the lower rim) is between 9.0 and 9.2 Å. By applying the SwissPDB viewer[77] a pore volume of 177 Å^3 was calculated. Most interestingly, these dimensions are somewhat larger than the 115 Å^3 we calculated for cucurbit[6]uril (**CB6**) with the same program, but comparable to those reported in literature (164 Å^3).[65] In

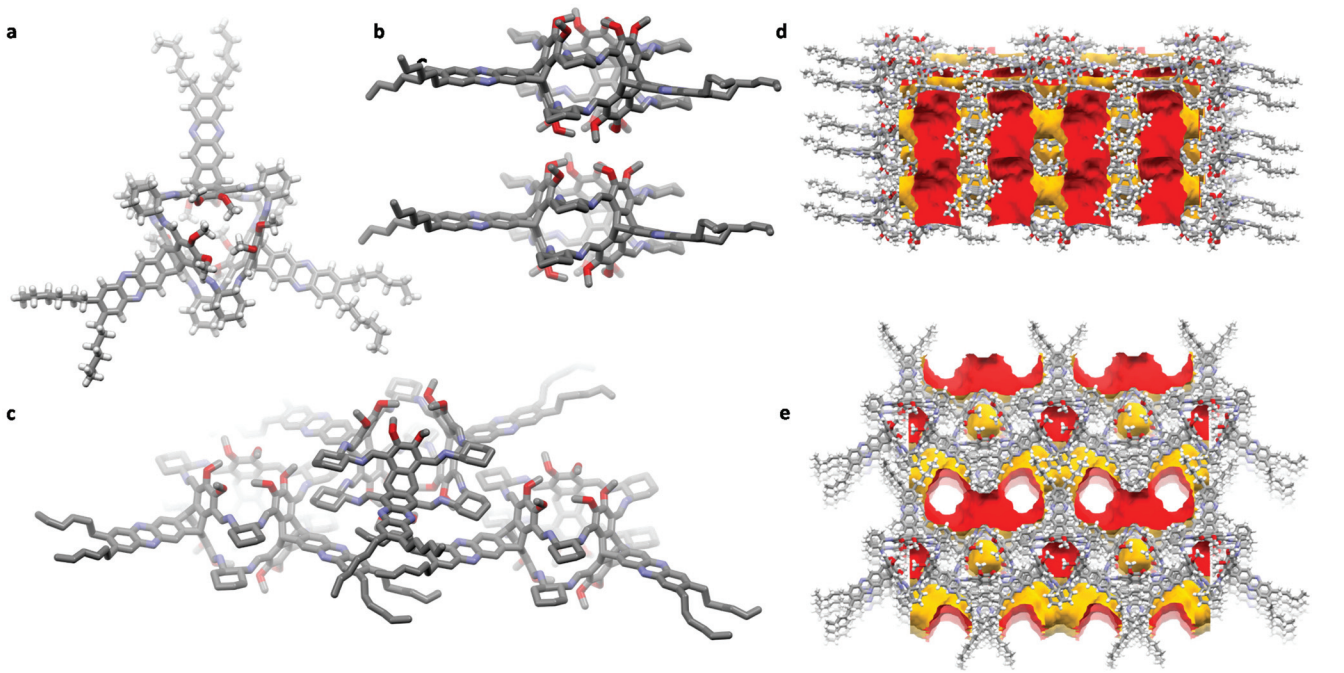

Fig. 4 Single crystal X-ray structure of cage (*R,R*)-**9**. (a) single molecule from top; (b) window-to-window packing; (c) packing by CH-π interactions of aromatic phenazine units and aliphatic cyclohexyl ring; (d) and (e) calculated pores with a probe radius of 1.82 Å. For (b) and (c) hydrogen atoms have been omitted for clarity. In (d) an (e) the red surface is the solvent accessible surface and yellow the inaccessible surface.

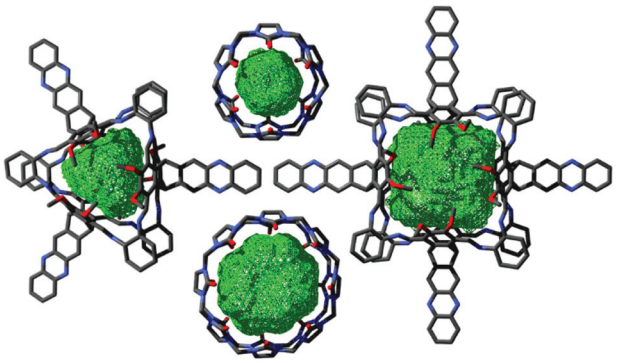

Fig. 5 Comparison of molecular pore volumes of cucurbitimines (*R,R*)-**9** (left) and (*R,R*)-**10** (right) with those of **CB6** (top middle) and **CB8** (bottom middle)., generated with SwissPDBviewer.[77] For details, see ESI.†

CB6 the diameter of two opposite oxygens at the rims is 3.9 Å, the inner distance of two opposite carbons is with 5.8 Å smaller than in cage **9** and the height is very similar (9.1 Å).

For the [4 + 8] cages **10** we were not successful to grow suitable crystals for a detailed analysis by X-ray diffraction. However, cage **9** is very rigid and thus shape-persistent and the experimental structure determined by X-ray diffraction fits nearly perfectly to the calculated model (PM6). Thus we take the PM6 model of the larger cage **10** for comparison with cucurbiturils. As in cucurbiturils the height is the same for all members of the family, the height is here also the same for cage **10** and cage **9** (9.1 Å). Due to the higher symmetry, the distance between two opposite oxygens at one rim can be measured. With 9.0 Å it is significantly larger than *e.g.* for cucurbituril[8] **CB8** (6.9 Å). The inner diameter (distance between two opposite triptycene bridgehead carbons) is 12.0 Å. The calculated void volume is with 368 Å^3 similar to what we estimated for **CB8** with the PDB viewer (351 Å^3) but substantially smaller than reported in literature (479 Å^3).[65] Furthermore we calculated the electron density distribution, which is similar to curcurbiturils, but less pronounced (see ESI†), so the curcubitimines may show a similar host–guest behaviour as the cucurbiturils.[65,66,78,79] Whereas all initial tests to incorporate ammonium compounds into the cavity did not show any uptake, it was realized that neutral molecules are found in the molecular void. As described above, by X-ray crystallography one DCM molecule was found in the interior of cage **9**, and as soon as it is purified by recycling-GPC with THF as eluent, one molecule of THF is bound inside, when analysed by ^{1}H NMR in toluene-d8 (Fig. 6). The peak at −0.84 ppm is clearly assigned to the eight THF protons of THF inside the cavity. The corresponding peaks of (*R,R*)-**9** of the host–guest complex are highlighted in blue. In Fig. 6 (top spectrum) already a second set of cage protons are detected (magenta colored peaks), that are shifted all slightly upfield. By time these increase in intensity (Fig. 6, bottom, whereas those of the THF@(*R,R*)-**9** complex decrease. Besides that, free THF is found (1.45 and 3.56 ppm), thus we conclude that THF most likely got exchanged by

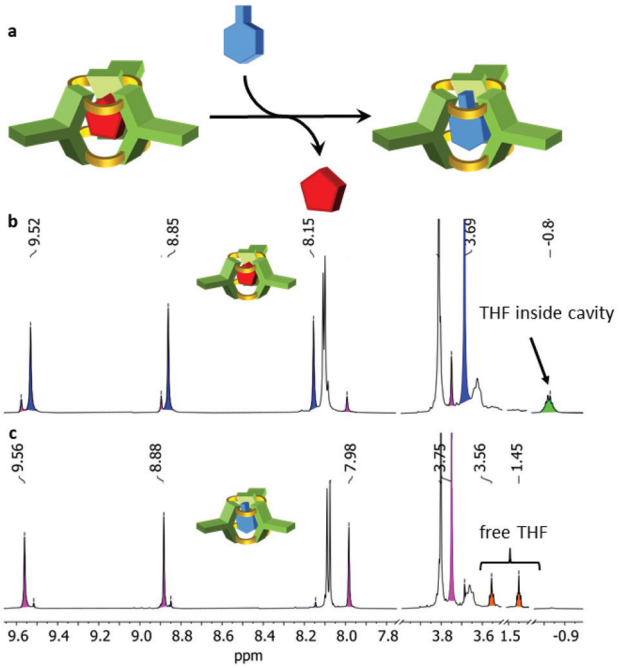

Fig. 6 (a) Exchange of host molecules from THF@(*R,R*)-**9** to toluene-d8@(*R,R*)-**9**. (b) ^{1}H NMR spectrum (700 MHz) of freshly prepared THF@(*R,R*)-**9** in toluene-d8. (c) same sample after exchange of THF guest by toluene-d8. Note, that in the upper spectrum some toluene-d8@(*R,R*)-**9** has formed.

toluene-d8. The exchange is very slow at room temperature (more than 2 d) but can be accelerated to less than 1 h at 100 °C.

Conclusions

Based on a triptycene tetraaldehyde a new type of imine cages has been introduced that have a similar shape than cucurbiturils. Therefore, these imine cages are named cucurbitimines. Initial studies demonstrate, that small neutral guests are bound inside the cavity and that their exchange (here THF by toluene) is kinetically suppressed due to the small window sizes of the opening. By increasing the temperature, the exchange of guest molecules can be accelerated. This behaviour is quite similar to that of the cucurbiturils. In contrast to those, the here discussed cucurbitimines are much better soluble in organic solvents and, which for cucubiturils is quite rare,[80] are chiral, opening up new possibilities for classical host–guest chemistry, but also for separation of volatile chiral compounds.[81] Furthermore, we will look for possibilities to get the larger members of the family ([5 + 10] and higher) to open up new vistas in supramolecular chemistry simply by enlarging the windows – as has been done before for cucurbiturils.

Conflicts of interest

There are no conflicts to declare.

Acknowledgements

We thank the European Research Council ERC in the frame of the consolidators grant CaTs n DOCs (grant no. 725765). Jochen C. Lauer and Tobias Kirschbaum (both Ruprecht-Karls-Universität Heidelberg) are acknowledged for their helpful discussions.

References

1 N. M. Rue, J. Sun and R. Warmuth, Polyimine Container Molecules and Nanocapsules, *Isr. J. Chem.*, 2011, **51**, 743–768.
2 V. Santolini, M. Miklitz, E. Berardo and K. E. Jelfs, Topological landscapes of porous organic cages, *Nanoscale*, 2017, **9**, 5280–5298.
3 M. Mastalerz, Porous Shape-Persistent Organic Cage Compounds of Different Size, Geometry, and Function, *ACC. Chem. Res.*, 2018, **51**, 2411–2422.
4 K. Acharyya and P. S. Mukherjee, Organic Imine Cages: Molecular Marriage and Applications, *Angew. Chem., Int. Ed.*, 2019, **58**, 8640–8653.
5 M. A. Little and A. I. Cooper, The Chemistry of Porous Organic Molecular Materials, *Adv. Funct. Mater.*, 2020, **30**, 1909842.
6 F. Beuerle and B. Gole, Covalent Organic Frameworks and Cage Compounds: Design and Applications of Polymeric and Discrete Organic Scaffolds, *Angew. Chem., Int. Ed.*, 2018, **57**, 4850–4878.
7 M. Mastalerz, Shape-Persistent Organic Cage Compounds by Dynamic Covalent Bond Formation, *Angew. Chem., Int. Ed.*, 2010, **49**, 5042–5053.
8 N. Christinat, R. Scopelliti and K. Severin, Multicomponent Assembly of Boronic Acid Based Macrocycles and Cages, *Angew. Chem.*, 2008, **120**, 1874–1878.
9 M. Hutin, G. Bernardinelli and J. R. Nitschke, An Iminoboronate Construction Set for Subcomponent Self-Assembly, *Chem. – Eur. J.*, 2008, **14**, 4585–4593.
10 N. Nishimura and K. Kobayashi, Self-Assembly of a Cavitand-Based Capsule by Dynamic Boronic Ester Formation, *Angew. Chem., Int. Ed.*, 2008, **47**, 6255–6258.
11 A. Granzhan, C. Schouwey, T. Riis-Johannessen, R. Scopelliti and K. Severin, Connection of Metallamacrocycles via Dynamic Covalent Chemistry: A Versatile Method for the Synthesis of Molecular Cages, *J. Am. Chem. Soc.*, 2011, **133**, 7106–7115.
12 J. Tönnemann, R. Scopelliti, K. O. Zhurov, L. Menin, S. Dehnen and K. Severin, Borophosphonate Cages: Easily Accessible and Constitutionally Dynamic Heterocubane Scaffolds, *Chem. – Eur. J.*, 2012, **18**, 9939–9945.
13 K. Ono, K. Johmoto, N. Yasuda, H. Uekusa, S. Fujii, M. Kiguchi and N. Iwasawa, Self-Assembly of Nanometer-Sized Boroxine Cages from Diboronic Acids, *J. Am. Chem. Soc.*, 2015, **137**, 7015–7018.
14 S. Klotzbach and F. Beuerle, Shape-Controlled Synthesis and Self-Sorting of Covalent Organic Cage Compounds, *Angew. Chem., Int. Ed.*, 2015, **54**, 10356–10360.
15 N. Schäfer, M. Bühler, L. Heyer, M. I. S. Röhr and F. Beuerle, Endohedral Hydrogen Bonding Templates the Formation of a Highly Strained Covalent Organic Cage Compound, *Chem. – Eur. J.*, 2021, **27**, 6077–6085.
16 S. Klotzbach, T. Scherpf and F. Beuerle, Dynamic covalent assembly of tribenzotriquinacenes into molecular cubes, *Chem. Commun.*, 2014, **50**, 12454–12457.
17 G. Zhang, O. Presly, F. White, I. M. Oppel and M. Mastalerz, A Permanent Mesoporous Organic Cage with an Exceptionally High Surface Area, *Angew. Chem., Int. Ed.*, 2014, **53**, 1516–1520.
18 S. M. Elbert, N. I. Regenauer, D. Schindler, W.-S. Zhang, F. Rominger, R. R. Schröder and M. Mastalerz, Shape-Persistent Tetrahedral [4+6] Boronic Ester Cages with Different Degrees of Fluoride Substitution, *Chem. – Eur. J.*, 2018, **24**, 11438–11443.
19 S.-W. Tam-Chang, J. S. Stehouwer and J. Hao, Formation of a Macrobicyclic Tris(disulfide) by Molecular Self-Assembly, *J. Org. Chem.*, 1999, **64**, 334–335.
20 K. R. West, K. D. Bake and S. Otto, Dynamic Combinatorial Libraries of Disulfide Cages in Water, *Org. Lett.*, 2005, **7**, 2615–2618.
21 J. Shin and K. Paek, *Bull. Korean Chem. Soc.*, 2014, **35**, 2205–2206.
22 C. Zhang, Q. Wang, H. Long and W. Zhang, A Highly C70 Selective Shape-Persistent Rectangular Prism Constructed through One-Step Alkyne Metathesis, *J. Am. Chem. Soc.*, 2011, **133**, 20995–21001.
23 Q. Wang, C. Zhang, B. C. Noll, H. Long, Y. Jin and W. Zhang, A Tetrameric Cage with D2 h Symmetry through Alkyne Metathesis, *Angew. Chem., Int. Ed.*, 2014, **53**, 10663–10667.
24 S. Lee, A. Yang, T. P. Moneypenny and J. S. Moore, Kinetically Trapped Tetrahedral Cages via Alkyne Metathesis, *J. Am. Chem. Soc.*, 2016, **138**, 2182–2185.
25 R.-C. Brachvogel, F. Hampel and M. von Delius, Self-assembly of dynamic orthoester cryptates, *Nat. Commun.*, 2015, **6**, 7129.
26 O. Shyshov, R.-C. Brachvogel, T. Bachmann, R. Srikantharajah, D. Segets, F. Hampel, R. Puchta and M. von Delius, Adaptive Behavior of Dynamic Orthoester Cryptands, *Angew. Chem., Int. Ed.*, 2017, **56**, 776–781.
27 M. Liu, M. A. Little, K. E. Jelfs, J. T. A. Jones, M. Schmidtmann, S. Y. Chong, T. Hasell and A. I. Cooper, Acid- and Base-Stable Porous Organic Cages: Shape Persistence and pH Stability via Post-synthetic "Tying" of a Flexible Amine Cage, *J. Am. Chem. Soc.*, 2014, **136**, 7583–7586.
28 X.-Y. Hu, W.-S. Zhang, F. Rominger, I. Wacker, R. R. Schröder and M. Mastalerz, Transforming a chemically labile [2+3] imine cage into a robust carbamate cage, *Chem. Commun.*, 2017, **53**, 8616–8619.
29 A. S. Bhat, S. M. Elbert, W.-S. Zhang, F. Rominger, M. Dieckmann, R. R. Schröder and M. Mastalerz,

Transformation of a [4+6] Salicylbisimine Cage to Chemically Robust Amide Cages, *Angew. Chem., Int. Ed.*, 2019, **58**, 8819–8823.

30 T. H. G. Schick, J. C. Lauer, F. Rominger and M. Mastalerz, Transformation of Imine Cages into Hydrocarbon Cages, *Angew. Chem., Int. Ed.*, 2019, **58**, 1768–1773.

31 P.-E. Alexandre, W.-S. Zhang, F. Rominger, S. M. Elbert, R. R. Schröder and M. Mastalerz, A Robust Porous Quinoline Cage: Transformation of a [4+6] Salicylimine Cage by Povarov Cyclization, *Angew. Chem., Int. Ed.*, 2020, **59**, 19675–19679.

32 M. Hähsler and M. Mastalerz, A Giant [8+12] Boronic Ester Cage with 48 Terminal Alkene Units in the Periphery for Postsynthetic Alkene Metathesis, *Chem. – Eur. J.*, 2021, **27**, 233–237.

33 S. Jiang, J. Bacsa, X. Wu, J. T. A. Jones, R. Dawson, A. Trewin, D. J. Adams and A. I. Cooper, Selective gas sorption in a [2+3] 'propeller' cage crystal, *Chem. Commun.*, 2011, **47**, 8919–8921.

34 M. W. Schneider, I. M. Oppel and M. Mastalerz, Exo-Functionalized Shape-Persistent [2+3] Cage Compounds: Influence of Molecular Rigidity on Formation and Permanent Porosity, *Chem. – Eur. J.*, 2012, **18**, 4156–4160.

35 K. Acharyya and P. S. Mukherjee, Hydrogen-Bond-Driven Controlled Molecular Marriage in Covalent Cages, *Chem. – Eur. J.*, 2014, **20**, 1646–1657.

36 P. Skowronek and J. Gawronski, Chiral Iminospherand of a Tetrahedral Symmetry Spontaneously Assembled in a [6+4] Cyclocondensation, *Org. Lett.*, 2008, **10**, 4755–4758.

37 T. Tozawa, J. T. A. Jones, S. I. Swamy, S. Jiang, D. J. Adams, S. Shakespeare, R. Clowes, D. Bradshaw, T. Hasell, S. Y. Chong, C. Tang, S. Thompson, J. Parker, A. Trewin, J. Bacsa, A. M. Z. Slawin, A. Steiner and A. I. Cooper, Porous organic cages, *Nat. Mater.*, 2009, **8**, 973–978.

38 N. Cao, Y. Wang, X. Zheng, T. Jiao and H. Li, Controllable Self-Assembly of Pills and Cages via Imine Condensation for Silver Cation Detection, *Org. Lett.*, 2018, **20**, 7447–7450.

39 T. Jiao, L. Chen, D. Yang, X. Li, G. Wu, P. Zeng, A. Zhou, Q. Yin, Y. Pan, B. Wu, X. Hong, X. Kong, V. M. Lynch, J. L. Sessler and H. Li, Trapping White Phosphorus within a Purely Organic Molecular Container Produced by Imine Condensation, *Angew. Chem., Int. Ed.*, 2017, **56**, 14545–14550.

40 J. C. Lauer, W.-S. Zhang, F. Rominger, R. R. Schröder and M. Mastalerz, Shape-Persistent [4+4] Imine Cages with a Truncated Tetrahedral Geometry, *Chem. – Eur. J.*, 2018, **24**, 1816–1820.

41 T. Kunde, E. Nieland, H. V. Schröder, C. A. Schalley and B. M. Schmidt, A porous fluorinated organic [4+4] imine cage showing CO_2 and H2 adsorption, *Chem. Commun.*, 2020, **56**, 4761–4764.

42 S. Hong, M. R. Rohman, J. Jia, Y. Kim, D. Moon, Y. Kim, Y. H. Ko, E. Lee and K. Kim, Porphyrin Boxes: Rationally Designed Porous Organic Cages, *Angew. Chem., Int. Ed.*, 2015, **54**, 13241–13244.

43 R. D. Mukhopadhyay, Y. Kim, J. Koo and K. Kim, Porphyrin Boxes, *Acc. Chem. Res.*, 2018, **51**, 2730–2738.

44 P. Wagner, F. Rominger, W.-S. Zhang, J. H. Gross, S. M. Elbert, R. R. Schröder and M. Mastalerz, Chiral Self-sorting of Giant Cubic [8+12] Salicylimine Cage Compounds, *Angew. Chem., Int. Ed.*, 2021, **60**, 8896–8904.

45 D. Xu and R. Warmuth, Edge-Directed Dynamic Covalent Synthesis of a Chiral Nanocube, *J. Am. Chem. Soc.*, 2008, **130**, 7520–7521.

46 H. Qu, Y. Wang, Z. Li, X. Wang, H. Fang, Z. Tian and X. Cao, Molecular Face-Rotating Cube with Emergent Chiral and Fluorescence Properties, *J. Am. Chem. Soc.*, 2017, **139**, 18142–18145.

47 M. E. Briggs, K. E. Jelfs, S. Y. Chong, C. Lester, M. Schmidtmann, D. J. Adams and A. I. Cooper, Shape Prediction for Supramolecular Organic Nanostructures: [4+4] Macrocyclic Tetrapods, *Cryt. Growth Des.*, 2013, **13**, 4993–5000.

48 M. Mastalerz, One-pot synthesis of a shape-persistent endo-functionalised nano-sized adamantoid compound, *Chem. Commun.*, 2008, 4756–4758, DOI: 10.1039/B808990F.

49 M. W. Schneider, I. M. Oppel, H. Ott, L. G. Lechner, H.-J. S. Hauswald, R. Stoll and M. Mastalerz, Periphery-Substituted [4+6] Salicylbisimine Cage Compounds with Exceptionally High Surface Areas: Influence of the Molecular Structure on Nitrogen Sorption Properties, *Chem. – Eur. J.*, 2012, **18**, 836–847.

50 M. W. Schneider, H.-J. S. Hauswald, R. Stoll and M. Mastalerz, A shape-persistent exo-functionalized [4+6] imine cage compound with a very high specific surface area, *Chem. Commun.*, 2012, **48**, 9861–9863.

51 Y. Liu, X. Liu and R. Warmuth, Multicomponent Dynamic Covalent Assembly of a Rhombicuboctahedral Nanocapsule, *Chem. – Eur. J.*, 2007, **13**, 8953–8959.

52 X. Liu and R. Warmuth, Solvent Effects in Thermodynamically Controlled Multicomponent Nanocage Syntheses, *J. Am. Chem. Soc.*, 2006, **128**, 14120–14127.

53 X. Liu, Y. Liu, G. Li and R. Warmuth, One-Pot, 18-Component Synthesis of an Octahedral Nanocontainer Molecule, *Angew. Chem., Int. Ed.*, 2006, **45**, 901–904.

54 J. Koo, I. Kim, Y. Kim, D. Cho, I.-C. Hwang, R. D. Mukhopadhyay, H. Song, Y. H. Ko, A. Dhamija, H. Lee, W. Hwang, S. Kim, M.-H. Baik and K. Kim, Gigantic Porphyrinic Cages, *Chem*, 2020, **6**, 3374–3384.

55 K. Su, W. Wang, S. Du, C. Ji, M. Zhou and D. Yuan, Reticular Chemistry in Construction of Porous Organic Cages, *J. Am. Chem. Soc.*, 2020, **142**, 18060–18072.

56 X. Wang, Y. Wang, H. Yang, H. Fang, R. Chen, Y. Sun, N. Zheng, K. Tan, X. Lu, Z. Tian and X. Cao, Assembled molecular face-rotating polyhedra to transfer chirality from two to three dimensions, *Nat. Commun.*, 2016, **7**, 12469.

57 H. Qu, X. Tang, X. Wang, Z. Li, Z. Huang, H. Zhang, Z. Tian and X. Cao, Chiral molecular face-rotating sandwich structures constructed through restricting the phenyl flipping of tetraphenylethylene, *Chem. Sci.*, 2018, **9**, 8814–8818.

58 A. G. Slater, M. A. Little, A. Pulido, S. Y. Chong, D. Holden, L. Chen, C. Morgan, X. Wu, G. Cheng, R. Clowes, M. E. Briggs, T. Hasell, K. E. Jelfs, G. M. Day and

A. I. Cooper, Reticular synthesis of porous molecular 1D nanotubes and 3D networks, *Nat. Chem.*, 2017, **9**, 17–25.

59 L. Zhang, L. Xiang, C. Hang, W. Liu, W. Huang and Y. Pan, From Discrete Molecular Cages to a Network of Cages Exhibiting Enhanced CO_2 Adsorption Capacity, *Angew. Chem., Int. Ed.*, 2017, **56**, 7787–7791.

60 C. Liu, K. Liu, C. Wang, H. Liu, H. Wang, H. Su, X. Li, B. Chen and J. Jiang, Elucidating heterogeneous photocatalytic superiority of microporous porphyrin organic cage, *Nat. Commun.*, 2020, **11**, 1047.

61 N. Sun, C. Wang, H. Wang, L. Yang, P. Jin, W. Zhang and J. Jiang, Multifunctional Tubular Organic Cage-Supported Ultrafine Palladium Nanoparticles for Sequential Catalysis, *Angew. Chem., Int. Ed.*, 2019, **58**, 18011–18016.

62 V. Abet, F. T. Szczypiński, M. A. Little, V. Santolini, C. D. Jones, R. Evans, C. Wilson, X. Wu, M. F. Thorne, M. J. Bennison, P. Cui, A. I. Cooper, K. E. Jelfs and A. G. Slater, Inducing Social Self-Sorting in Organic Cages To Tune The Shape of The Internal Cavity, *Angew. Chem., Int. Ed.*, 2020, **59**, 16755–16763.

63 W. A. Freeman, W. L. Mock and N. Y. Shih, Cucurbituril, *J. Am. Chem. Soc.*, 1981, **103**, 7367–7368.

64 J. Kim, I.-S. Jung, S.-Y. Kim, E. Lee, J.-K. Kang, S. Sakamoto, K. Yamaguchi and K. Kim, New Cucurbituril Homologues: Syntheses, Isolation, Characterization, and X-ray Crystal Structures of Cucurbit[n]uril (n=5, 7, and 8), *J. Am. Chem. Soc.*, 2000, **122**, 540–541.

65 J. W. Lee, S. Samal, N. Selvapalam, H.-J. Kim and K. Kim, Cucurbituril Homologues and Derivatives: New Opportunities in Supramolecular Chemistry, *Acc. Chem. Res.*, 2003, **36**, 621–630.

66 S. J. Barrow, S. Kasera, M. J. Rowland, J. del Barrio and O. A. Scherman, Cucurbituril-Based Molecular Recognition, *Chem. Rev.*, 2015, **115**, 12320–12406.

67 E. Masson, X. Ling, R. Joseph, L. Kyeremeh-Mensah and X. Lu, Cucurbituril chemistry: a tale of supramolecular success, *RSC Adv.*, 2012, **2**, 1213–1247.

68 X. Sun, B. Liu, Q. Wu and F. Li, Photochemical properties and interfacial fluorescence sensing for homocysteine of triptycene orthoquinone layer-by-layer-assembled multilayers, *Thin Solid Films*, 2014, **562**, 603–607.

69 J.-M. Zhao, H.-Y. Lu, J. Cao, Y. Jiang and C.-F. Chen, Highly selective synthesis of triptycene o-quinone derivatives and their optical and electrochemical properties, *Tetrahedron Lett.*, 2009, **50**, 219–222.

70 K. Baumgärtner, F. Rominger and M. Mastalerz, An Oxidative Macrobicyclic Ring Opening of a Triptycene to a Highly Functionalized Fluorene Derivative, *J. Org. Chem.*, 2015, **80**, 8881–8886.

71 F. Zhang, S. Bai, G. P. A. Yap, V. Tarwade and J. M. Fox, Abiotic Metallofoldamers as Electrochemically Responsive Molecules, *J. Am. Chem. Soc.*, 2005, **127**, 10590–10599.

72 K. Baumgärtner, M. Hoffmann, F. Rominger, S. M. Elbert, A. Dreuw and M. Mastalerz, Homoconjugation and Intramolecular Charge Transfer in Extended Aromatic Triptycenes with Different π-Planes, *J. Org. Chem.*, 2020, **85**, 15256–15272.

73 T. Hasell, S. Y. Chong, K. E. Jelfs, D. J. Adams and A. I. Cooper, Porous Organic Cage Nanocrystals by Solution Mixing, *J. Am. Chem. Soc.*, 2012, **134**, 588–598.

74 B. Teng, M. A. Little, T. Hasell, S. Y. Chong, K. E. Jelfs, R. Clowes, M. E. Briggs and A. I. Cooper, Synthesis of a Large, Shape-Flexible, Solvatomorphic Porous Organic Cage, *Cryt. Growth Des.*, 2019, **19**, 3647–3651.

75 L. Ueberricke, D. Holub, J. Kranz, F. Rominger, M. Elstner and M. Mastalerz, Triptycene End-Capped Quinoxalinophenanthrophenazines (QPPs): Influence of Substituents and Conditions on Aggregation in the Solid State, *Chem. – Eur. J.*, 2019, **25**, 11121–11134.

76 D. Holden, K. E. Jelfs, A. Trewin, D. J. Willock, M. Haranczyk and A. I. Cooper, Gas Diffusion in a Porous Organic Cage: Analysis of Dynamic Pore Connectivity Using Molecular Dynamics Simulations, *Phys. Chem. C*, 2014, **118**, 12734–12743.

77 N. Guex and M. C. Peitsch, SWISS-MODEL and the Swiss-Pdb Viewer: An environment for comparative protein modeling, *ELECTROPHORESIS*, 1997, **18**, 2714–2723.

78 W. L. Mock and N. Y. Shih, Host-guest binding capacity of cucurbituril, *J. Org. Chem.*, 1983, **48**, 3618–3619.

79 J. Lagona, P. Mukhopadhyay, S. Chakrabarti and L. Isaacs, The Cucurbit[n]uril Family, *Angew. Chem., Int. Ed.*, 2005, **44**, 4844–4870.

80 W.-H. Huang, P. Y. Zavalij and L. Isaacs, Chiral Recognition inside a Chiral Cucurbituril, *Angew. Chem., Int. Ed.*, 2007, **46**, 7425–7427.

81 T. Mitra, K. E. Jelfs, M. Schmidtmann, A. Ahmed, S. Y. Chong, D. J. Adams and A. I. Cooper, Molecular shape sorting using molecular organic cages, *Nat. Chem.*, 2013, **5**, 276.

